http://dx.doi.org/10.5012/bkcs.2013.34.10.2925

Molecular Dynamics Simulation Study for Hydroxide Ion in Supercritical Water using SPC/E Water Potential

Song Hi Lee

Department of Chemistry, Kyungsung University, Busan 608-736, Korea. E-mail: shlee@ks.ac.kr
Received May 30, 2013, Accepted July 9, 2013

We present results of molecular dynamics simulations for hydroxide ion in supercritical water of densities 0.22, 0.31, 0.40, 0.48, 0.61, and 0.74 g/cc using the SPC/E water potential with Ewald summation. The limiting molar conductance of OH^- ion at 673 K monotonically increases with decreasing water density. It is also found that the hydration number of water molecules in the first hydration shells around the OH^- ion decreases and the potential energy per hydrated water molecule also decreases in the whole water density region with decreasing water density. Unlike the case in our previous works on LiCl, NaCl, NaBr, and CsBr [Lee *at al*., *Chem. Phys. Lett.* **1998**, *293*, 289-294 and *J. Chem. Phys.* **2000**, *112*, 864-869], the number of hydrated water molecules around ions and the potential energy per hydrated water molecule give the same effect to cause a monotonically increasing of the diffusion coefficient with decreasing water density in the whole water density region. The decreasing residence times are consistent with the decreasing potential energy per hydrated water molecule.

Key Words : OH^- ion mobility, Supercritical water, Molecular dynamics simulation, SPC/E water model

Introduction

In the mid of 1990, there were two experimental results for the limiting molar conductances of ions as a function of the density of water at supercritical states. One displayed a clear change of slope from the assumed linear dependence of LiCl, NaCl, NaBr, and CsBr on the water density by Wood *et al.*[1] and the other had a clear maximum in limiting molar conductance of NaOH by Ho and Palmer.[2]

In the previous works,[3,4] we reported molecular dynamics (MD) simulations of NaCl, LiCl, NaBr, and CsBr in supercritical water aimed at explaining experimental observations of limiting molar conductance as a function of the water density at supercritical state points using the SPC/E model[5] for water and literature-derived ion-water potential parameters. We explained the experimental observations in terms of a changing balance between two competing factors - the effect of the number of hydrated water molecules around ions and the interaction strength between the ions and the hydrated water molecules. The number of hydrated water molecules around ions was the dominating factor in the higher-density region while the interaction between the ions and the hydrated water molecules dominated in the lower-density region. The competition between these two factors was evident in the residence times of water in the first hydration shells around the ions.

The difference of limiting molar conductance between NaCl and NaOH at supercritical water was originated apparently from the difference of conductance between Cl^- and OH^- at ambient state for the same count ion Na^+, as shown in Figure 1, which compared the experimental measures of limiting molar conductances of Cl^- and OH^- as a function of water density. The assumed limiting molar conductance of F^- is also shown in Figure 1. If one considers only the size effect of ion on the limiting molar conductance, the size of OH^- is similar to that of F^- and it is expected that the limiting molar conductance of OH^- is similar to that of F^- and is smaller than that of Cl^-, but the molar conductance of OH^- (199.1 $S{\cdot}cm^2/mol$) is much larger than those of F^- (55.4) and Cl^- (76.4) at ambient state. This tells us there is other important factor on the limiting molar conductance of OH^- beside the size effect of ion – called the Grotthuss mechanism.

The large difference of the limiting molar conductance between H^+ and other monovalent cations at ambient water is also found in that between OH^- and other monovalent anions. The transport of H^+ in water is well known as the Grotthuss chain mechanism that does not involves its actual motion through the solution. Instead of a single, highly solvated proton moving through the solution, it is believed

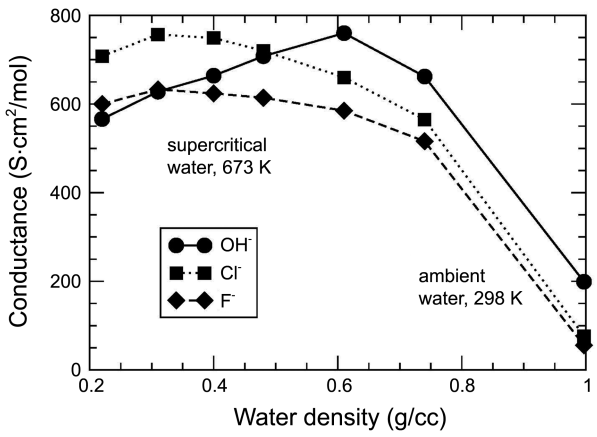

Figure 1. Limiting molar conductances of OH^-, Cl^-, and F^- (assumed) ions as a function of water density in supercritical water and ambient water.

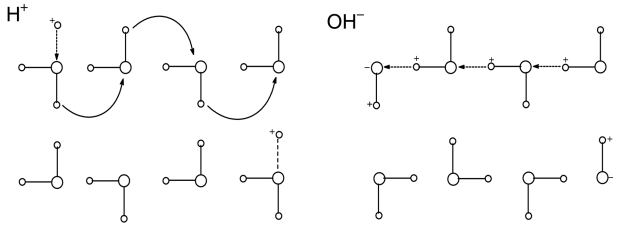

Figure 2. Grotthuss chain mechanisms.

that there is an effective motion of a proton which involves the rearrangement of bonds through a long chain of water molecules as shown Figure 2(a). A closer insight into the transport of OH^- reveals that the large value of the limiting molar conductance of OH^- is also related to the Grotthuss chain mechanism as shown Figure 2(b) in addition to its actual motion through the solution. The same and opposite directions of H^+ transfer in the movements of H^+ and OH^- is called "dynamic asymmetry".[6]

In this paper, we report the results of our molecular dynamics (MD) simulations for the limiting molar conductances of OH^- in supercritical water at 673 K using the SPC/E model. The paper is organized as follows. Section II contains a brief description of molecular models and MD simulation methods followed by section III, which presents the results and discussion of our simulations, and our conclusions are summarized in section IV.

Molecular Model and Molecular Dynamics Simulation

The SPC/E (extended simple point charge) model[5] was adopted for the interactions between water molecules and between ion and water molecules. The pair potential between ion and water has the form

$$v_{iw} = 4\varepsilon_{io}\left[\left(\frac{\sigma_{io}}{r_{io}}\right)^{12} - \left(\frac{\sigma_{io}}{r_{io}}\right)^{6}\right] + \Sigma_{k\in i}\Sigma_{l\in w}\frac{q_k q_l}{r_{kl}}, \qquad (1)$$

where σ_{io} and ε_{io} are Lennard-Jones (LJ) parameters between the center of mass of ion i and oxygen on a water molecule, q_k is the charge at site k in ion, and q_l is the charge at site l in water. Also, r_{io} and r_{kl} are the distances between the center of mass of ion i and the oxygen site of a water molecule and between the site k in ion and the site l in water. The hydroxide ion-water σ_{io} and ε_{io} are 3.060 Å and 0.5771 kJ/mol,[7] respectively. The electrostatic charges on the oxygen and hydrogen atoms of the hydroxide ion are chosen as −0.8476 e and 0.4238 e (Sim.1) which are the same on the SPCE water molecule. The other choice is −2 e and +1 e (Sim.2) as used for monovalent ions in the previous studies.[3,4]

The experimental critical properties of water are T_c = 647.13 K, ρ_c = 0.322 g/cm^3, and P_c = 220.55 bar,[8] and the critical properties of SPC/E water are T_c = 640 K, ρ_c = 0.29 g/cm^3, and P_c = 160 bar.[9] We have chosen the simulation state points for the calculation of the limiting molar conductance of OH^- ion at the reduced temperature, $T_r = T/T_c$ = 1.05 (673 K) and at the reduced densities, $\rho_r = \rho/\rho_c$ = 0.76, 1.07, 1.38, 1.66, 2.10, and 2.55, corresponding to real densities of about 0.22, 0.31, 0.40, 0.48, 0.61, and 0.74 g/cm^3 for the SPC/E model; this spans the range of densities around 0.45 g/cm^3, where the clear change of slope from the assumed linear dependence of limiting molar conductances of LiCl, NaCl, NaBr, and CsBr on density[1] and the maximum in limiting molar conductance of NaOH are located.[2]

Each MD simulation of a single OH^- ion with 215 SPC/E water molecules was carried out in the NVT ensemble, and the density was fixed at a given density above, which corresponds to a cubic box length of L = 30.85, 27.52, 25.28, 23.87, 21.96, and 20.59 Å. A stationary Na^+ counterion which interacts with O and H atoms by electrostatic and Lennard-Jones interactions, was introduced at a corner of the cubic simulation box to maintain electro-neutrality.[10] The usual periodic boundary condition in the x-, y-, and z-directions and the minimum image convention for pair potential were applied. Gaussian kinetics[11-13] was used to control the temperature, and a quaternion formulation[14,15] was employed to solve the equations of rotational motion about the center of mass of rigid SPC/E water molecules and OH^- ion. Gear's fifth-order predictor-corrector algorithm[16] with a time step of 1 fs served to integrate the equations of motion. Ewald summations were used in our simulations with the parameter for κ = 5.0/L and the real-space cut distance r_{cut} and K_{max} chosen as 0.5L and 7, respectively. MD runs of 2,000,000 time steps each were needed for the ion-water system to reach equilibrium. The equilibrium properties were then averaged over 5 blocks of 1,000,000 time steps (1 ns) for a total of 5,000,000 (5 ns). The configurations of molecules were stored every five time steps for further analysis.

The diffusion coefficient, D, of OH^- ion is calculated from the mean square displacement (MSD) and from the velocity autocorrelation function (VAC), and the ion mobility is obtained by $u = D\ z\ e/kB\ T = D\ z\ F/RT$ (Einstein relation), where kB is the Boltzmann constant, R is the gas constant, F is the Faraday constant, zi is the charge on the ion in units of the electronic charge e, and T is the absolute temperature. The limiting molar conductance of OH^- ion can be calculated from $\lambda^o = u\ z\ F$.

Results and Discussion

The summaries of diffusion coefficients of OH^- ion and water, ion-water and water-water potential energies, hydration numbers, and residence times of water in the first hydration number are listed in Table 1 for q_O = −0.8476 e and q_H = +0.4238 e for OH^- ion (Sim.1) and in Table 2 for q_O = −2 e and q_H = +1 e for OH^- ion (Sim.2), respectively.

The radial distribution functions, $g_{io}(r)$, for the OH^- ion and the O atoms of water molecules are shown in Figure 3 for q_O = −0.8476 e and q_H = +0.4238 e for OH^- ion (Sim.1) and in Figure 4 for q_O = −2 e and q_H = +1 e for OH^- ion

Table 1. Average diffusion coefficient (10^{-5} cm^2/s) of OH^- ion, OH^- ion-water potential energy (kJ/mol), hydration number, ion-water potential energy divided by hydration number, residence time of water (ps), water-water potential energies (kJ/mol), and diffusion coefficient (10^{-5} cm^2/s) of water calculated from the MSD at 673 K and 298 K (0.997 g/cc) using $q_O = -0.8476$ *e* and $q_H = +0.4238$ *e* for OH^- ion (Sim.1)

Density (g/cc)	D_{OH-}	Ion-water PE	Hydration number (n)	Ion-water PE/n	Residence time of water	Water-water PE	D_w
0.22	87.1±6.2	-122.5±9.9	3.31±0.14	-37.0	0.84±0.02	-10.5±0.0	132.2±0.6
0.31	71.1±5.9	-136.5±7.1	3.67±0.13	-37.2	0.85±0.01	-13.3±0.0	98.3±1.0
0.40	69.6±7.0	-147.3±6.1	3.94±0.12	-37.4	0.86±0.01	-15.5±0.0	78.6±0.3
0.48	61.5±8.6	-155.8±5.6	4.15±0.13	-37.5	0.86±0.01	-17.3±0.0	65.9±0.4
0.61	50.1±2.2	-168.3±5.5	4.49±0.12	-37.5	0.87±0.01	-20.2±0.0	50.1±0.3
0.74	43.1±3.5	-180.5±5.4	4.78±0.11	-37.8	0.88±0.01	-22.8±0.0	38.6±0.2
0.997	30.7±2.7	-203.6±4.2	4.90±0.10	-41.6	1.07±0.01	-27.1±0.0	22.1±0.1
298 K	2.75±0.1	-255.6±4.0	4.93±0.08	-51.8	7.78±0.23	-40.7±0.0	2.62±0.02

Table 2. Average diffusion coefficient (10^{-5} cm^2/s) of OH^- ion, OH^- ion-water potential energy (kJ/mol), hydration number, ion-water potential energy divided by hydration number, residence time of water (ps), water-water potential energies (kJ/mol), and diffusion coefficient (10^{-5} cm^2/s) of water calculated from the MSD at 673 K and 298 K (0.997 g/cc) using $q_O = -2$ *e* and $q_H = +1$ *e* for OH^- ion (Sim.2)

Density (g/cc)	D_{OH-}	Ion-water PE	Hydration number (n)	Ion-water PE/n	Residence time of water	Water-water PE	D_w
0.22	17.6±1.3	-998.5±8.1	6.16±0.17	-162	4.56±0.03	-10.0±0.0	121.3±0.4
0.31	15.2±1.3	-1035±10	6.20±0.18	-167	4.66±0.02	-12.6±0.0	93.2±0.3
0.40	15.0±1.3	-1059±10	6.25±0.17	-169	4.70±0.01	-14.8±0.0	75.4±0.3
0.48	13.8±0.9	-1072±11	6.30±0.15	-170	4.74±0.02	-16.5±0.0	63.7±0.2
0.61	12.2±0.6	-1094±11	6.36±0.16	-172	4.87±0.01	-19.2±0.0	48.7±0.3
0.74	10.4±0.4	-1115±12	6.43±0.09	-173	5.01±0.02	-21.8±0.0	37.4±0.3
0.997	7.91±0.7	-1170±12	6.61±0.08	-177	5.52±0.01	-26.0±0.0	21.7±0.1
298 K	0.62±0.1	-1328±8	6.86±0.04	-194	94.0±0.3	-39.4±0.0	2.31±0.01

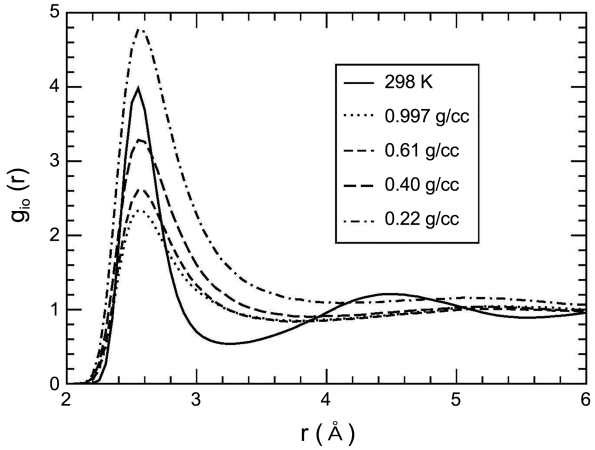

Figure 3. Radial distribution functions $g_{io}(r)$ of SPC/E water molecules as a function of the distance r(Å) between OH^- (*i*) and oxygen atom(*o*) of a water molecule using $q_O = -0.8476$ *e* and $q_H = +0.4238$ *e* for OH^- ion at 298 K (0.997 g/cc) and 673 K (0.997, 0.61, 0.40, and 0.22 g/cc).

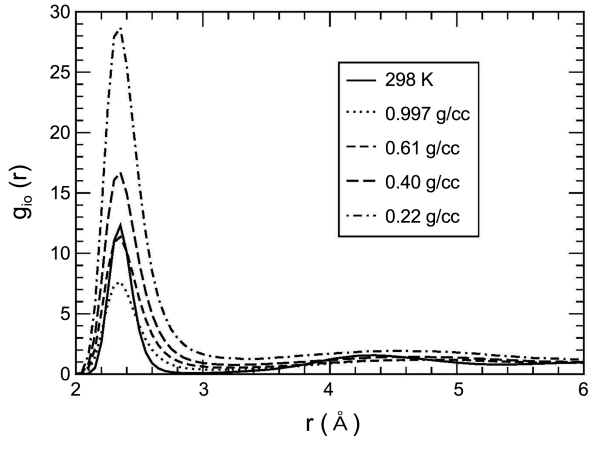

Figure 4. Radial distribution functions $g_{io}(r)$ of SPC/E water molecules as a function of the distance r(Å) between OH^- (*i*) and oxygen atom(*o*) of a water molecule using $q_O = -2$ *e* and $q_H = +1$ *e* for OH^- ion at 298 K (0.997 g/cc) and 673 K (0.997, 0.61, 0.40, and 0.22 g/cc).

(Sim.2), respectively. In Figure 3 the $g_{io}(r)$ at 298 K has the clear first and second peaks with the position of the first minimum at 3.25 Å but at 673 K the first peaks become broader with the positions of the first minima at 3.8-4.0 Å as water density increases and the second peaks are not clear. When the electrostatic charges on the O and H atoms of the OH^- ion are increased (Sim.2), though the change of the first peaks with water density in Sim.2 is somewhat similar to Sim.1, the clear broad second peaks exist at 673 K. The widths of the first peaks are smaller (2.95 Å at 298 K and 3.2-3.4 Å at 673 K) than those in Sim.1 due to the strong electrostatic potential between the OH^- ion and water molecules, even though the hydration numbers in the first hydration shells in Sim.2 are equal or less than those in

Sim.1.

The hydration number n in the first hydration shell is calculated from the ion-oxygen distribution functions $g_{io}(r)$ using

$$n = \rho_w \int_0^{R_1} g_{io}(r)\, 4\pi r^2\, dr\,, \qquad (2)$$

where ρ_w is the bulk number density of water and the upper limit of integration R_1 is the radius of the first hydration sphere which corresponds to the first minimum in $g_{io}(r)$. The size of hydrated ion is often measured by the first minimum in $g_{io}(r)$. Table 1 and 2 list the hydration numbers of water molecules in the first hydration shells around the OH^- ion for Sim.1 and Sim.2, respectively. These numbers decrease with decreasing water density at 673 K. This observation is agreed when compared with those in the cases of Cl^- ion[3] and Br^- ion[4], but the hydration numbers at 673 K around Cl^- and Br^- ions are in the range 6.8-8.6 and 7.3-9.5, compared with OH^- ion of 3.3-4.8 for Sim.1 and 6.2-6.6 for Sim.2.

In Figures 5 and 6 we display the snapshots of equilibrium configurations of water molecules around OH^- ion within 5 Å for Sim.1 and Sim.2 at (a) 298 K and (b) at 673 K and 0.48 g/cc. The pictures describe the clear chemical environment around the OH^- ion for each case. While the OH^- ion for Sim.1 at 298 K has five hydrogen- (H-) bonds (4.9 hydration number in the first hydration shell of 3.25 Å in Table 1), four accepted and one donated, it is remarkable that only two H-bonds appears around the OH^- ion at 673 K and 0.48 g/cc even though the hydration number is equal to 4.2 in the first hydration shell of 3.8-4.0 Å listed in Table 1. This indicates that the water molecules in the first hydration shell around the OH^- ion at supercritical states are weakly bounded to the OH^- ion due to the small electrostatic charges on the O and H atoms of the OH^- ion for Sim.1 as seen in the ion-water potential energy divided by hydration number listed in Table 1.

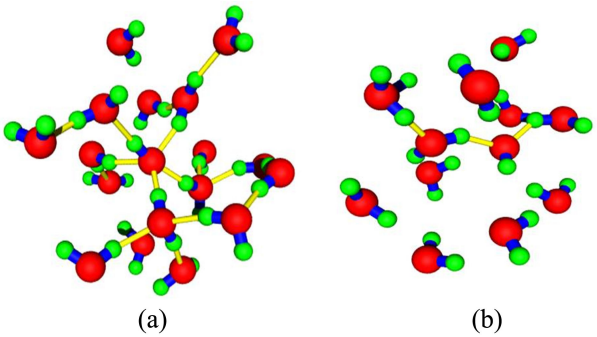

Figure 5. Snapshots of equilibrium configurations of SPC/E water molecules around OH^- ion within 5 Å using $q_O = -0.8476\ e$ and $q_H = +0.4238\ e$ for OH^- ion (Sim.1) at (a) T = 298 K and (b) at T = 673 K and ρ = 0.48 g/cc.

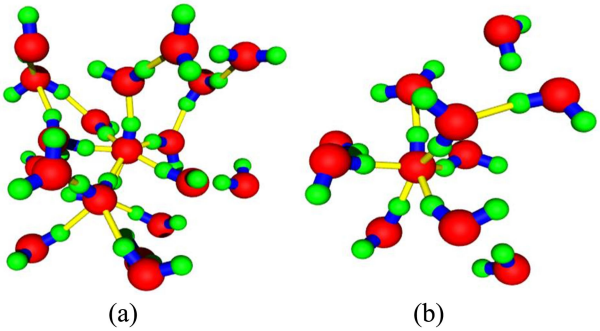

Figure 6. Snapshots of equilibrium configurations of SPC/E water molecules around OH^- ion within 5 Å using $q_O = -2\ e$ and $q_H = +1\ e$ for OH^- ion (Sim.2) at (a) T = 298 K and (b) at T = 673 K and ρ = 0.48 g/cc.

When the electrostatic charges on the O and H atoms of the OH^- ion are increased (Sim.2), the OH^- ion at 298 K has seven H-bonds (6.9 hydration number in the first hydration shell of 2.95 Å in Table 2), six accepted and one donated, but unlike Sim.1 the number of the H-bonds at 673 K and 0.48 g/cc is six, five accepted and one donated, and the hydration number (6.3) in the first hydration shells of 3.2-3.4 Å in Sim.2 are 1.5 times that (4.2) in Sim.1. One observes that the water molecules in the first hydration shell around the OH^- ion at supercritical states are strongly bounded to the OH^- ion due to the large electrostatic charges on the O and H atoms of the OH^- ion for Sim.2 as seen in the ion-water potential energy divided by hydration number listed in Table 2.

The diffusion coefficients, D, calculated from the mean square displacements (MSD) of OH^- ion are compared, in Figure 7, with the experimental results. D and its error bar estimate of OH^- ion was obtained from the averaged MSDs over 5 blocks of 1,000,000 time steps and the MSD of OH^- ion (not shown) shows a straight line as a function of time. As the water density at 673 K decreases, two sets of D results using $q_O = -0.8476\ e$ and $q_H = +0.4238\ e$ for OH^- ion (Sim.1) and $q_O = -2\ e$ and $q_H = +1\ e$ for OH^- ion (Sim.2) are monotonically increased, neither displaying a clear change of slope from the assumed linear dependence such as LiCl, NaCl, NaBr, and CsBr reported by Wood *et al.*[1] nor having a clear maximum in limiting molar conductance of NaOH by

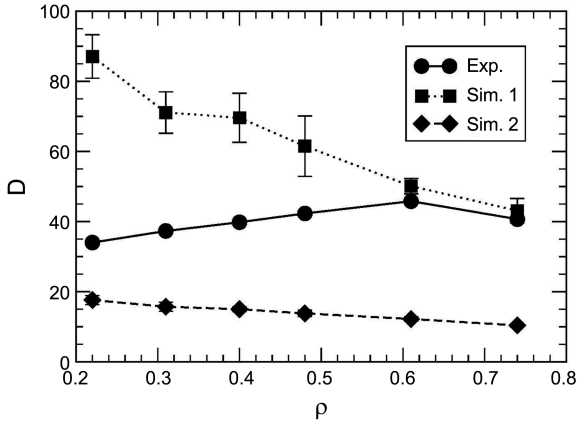

Figure 7. Comparison of diffusion coefficients D(10^{-5} cm^2/s) of OH^- ion as a function water density (g/cc) calculated from the mean square displacement from MD simulations (Sim.1 ■: using $q_O = -0.8476\ e$ and $q_H = +0.4238\ e$ for OH^- ion, and Sim.2 ◆: using $q_O = -0.8476\ e$ and $q_H = +0.4238\ e$ for OH^- ion) with the experimental values (●). The error bars indicate the standard deviation.

Ho and Palmer.[2] The explanation for this behavior of D of OH^- ion at supercritical states follows.

In Table 1 and 2, the average ion-water potential energy at 673 K decreases with decreasing water density for both Sim.1 and Sim.2 simulations as observed in the studies of Cl^- ion[3] and Br^- ion[4]. However, the potential energy per hydrated water molecule, defined as the average ion-water energy divided by the hydration number, also decreases with decreasing water density for both Sim.1 and Sim.2 simulations even though both the average ion-water potential energy and the hydration number decreases with decreasing water density at 673 K. This observation is the opposite trend reported in the studies of Cl^- ion[3] and Br^- ion[4]. As discussed in section I, there exists a changing balance between two competing factors in the explanation of experimental observations of limiting molar conductances of NaCl, LiCl, NaBr, and CsBr as a function of the water density at supercritical state points - the effect of the number of hydrated water molecules around ions and the interaction strength between the ions and the hydrated water molecules. The number of hydrated water molecules around ions was the dominating factor in the higher-density region while the interaction between the ions and the hydrated water molecules dominated in the lower-density region. However, in the case of OH^- ion, the hydration number of water molecules in the first hydration shells around the OH^- ion decreases and the potential energy per hydrated water molecule also decreases in the whole water density region with decreasing water density. Since there is no balance between two competition factors, instead the number of hydrated water molecules around ions and the potential energy per hydrated water molecule give the same effect to cause a monotonically increasing of the diffusion coefficient with decreasing water density in the whole water density region.

Next, we discuss the residence time for the hydrated SPC/E water molecules in the hydration shells of OH^- ion. The residence times are calculated from time correlation functions[17,18] defined by

$$R(r,t) = \frac{1}{N_r}\Sigma_{i=1}^{N_r}[\theta_i(r,0)\cdot\theta_i(r,t)] \quad (3)$$

where $\theta_i(r,t)$ is the Heaviside unit step function, which is 1 if a water molecule i is in a region r within the coordination shell of the ion at time t and zero otherwise, and N_r is the average number of water molecules in this region r at t = 0. Figures 8 and 9 show the time dependence of R(r,t) for water in the first solvation shell alone for Sim.1 and Sim.2, respectively, as a function of time calculated from our simulations. The residence time, τ, is obtained by fitting the time correlation function to an exponential decay $\langle R(r,t)\rangle \approx \exp(-t/\tau)$, which is useful particularly when τ is large.

The residence times, also listed in Tables 1 and 2, show the average decay times of water in the first shell alone. We note that these times decrease with decreasing water density at 673 K which gives another striking when compared with those in the cases of Cl^- ion[3] and Br^- ion[4], in which τ increases with decreasing water density. The residence times

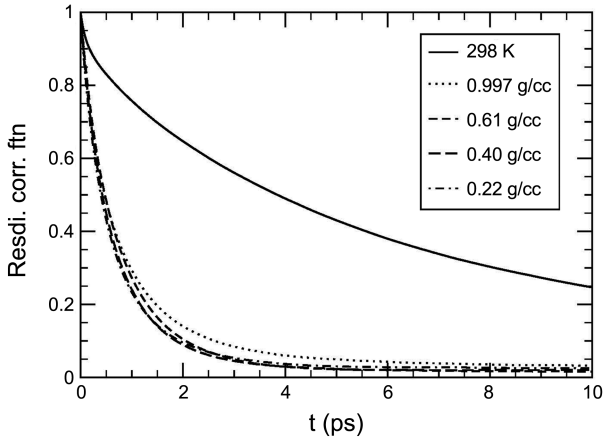

Figure 8. Residence time correlation function for the hydrated SPC/E water molecules in the first hydration shell of OH^- ion using $q_O = -0.8476\ e$ and $q_H = +0.4238\ e$ for OH^- ion (Sim.1) at 298 K (0.997 g/cc) and 673 K (0.997, 0.61, 0.40, and 0.22 g/cc) at 298 K (0.997 g/cc) and 673 K (0.997, 0.61, 0.40, and 0.22 g/cc).

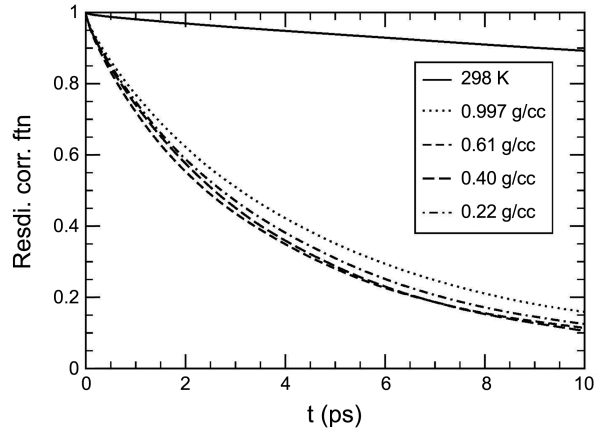

Figure 9. Residence time correlation function for the hydrated SPC/E water molecules in the first hydration shell of OH^- ion using $q_O = -2\ e$ and $q_H = +1\ e$ for OH^- ion (Sim.2) at 298 K (0.997 g/cc) and 673 K (0.997, 0.61, 0.40, and 0.22 g/cc).

at 673 K around Cl^- and Br^- ions are in the range 1.5-1.9 ps and 1.7-2.1 ps, compared with OH^- ion of 0.84-0.88 for Sim.1 and 4.6-5.0 for Sim.2. The less residence times in the lower-density region are consistent with the weaker potential energy per hydrated water molecule than in the higher-density region, which causes a monotonically increasing of D with decreasing water density in the whole water density region.

The average potential energies of water-water listed in Tables 1 (Sim.1) and 2 (Sim.2) decrease with decreasing water density at 673 K due to increasing water-water distance in which the potential energy for water includes a polarization correction[5] of 5.2 kJ/mol. The water-water potential energies for Sim.1 are greater than those for Sim.2 which indicates less influenced by the OH^- ions due to the small electrostatic charges on the O and H atoms of the OH^- ion. The evidence for the lesser influence on bulk water by the OH^- ion in solution is also apparent in the diffusion coefficient of water

listed in Tables 1 (Sim.1) and 2 (sim.2) showing that D_w in Sim.1 is greater than those in Sim.2.

Conclusion

We have carried out a series of molecular dynamics simulations of model OH^- ion-water systems at supercritical states using SPC/E water model and Ewald summation. We have chosen two sets of the electrostatic charge of the OH^- ion; $q_O = -0.8476\ e$ and $q_H = +0.4238\ e$ (Sim.1) and $q_O = -2\ e$ and $q_H = +1\ e$ (Sim.2). The diffusion coefficients, D, calculated from the mean square displacements of OH^- ion in Sim.1 and Sim.2 are monotonically increased with decreasing water density at 673 K, neither displaying a clear change of slope from the assumed linear dependence such as LiCl, NaCl, NaBr, and CsBr reported by Wood *et al.*[1] nor having a clear maximum in limiting molar conductance of NaOH by Ho and Palmer.[2] The potential energy per hydrated water molecule also decreases with decreasing water density for both Sim.1 and Sim.2 simulations even though both the average ion-water potential energy and the hydration number decreases with decreasing water density at 673 K. Unlike the previous studies of limiting molar conductances of NaCl, LiCl, NaBr, and CsBr,[3,4] there is no balance between two competition factors, instead the number of hydrated water molecules around ions and the potential energy per hydrated water molecule give the same effect to cause a monotonically increasing of the diffusion coefficient with decreasing water density in the whole water density region. The less residence times in the lower-density region are consistent with the weaker potential energy per hydrated water molecule than in the higher-density region.

One can find the evidence of the Grotthuss chain mechanism for OH^- ion in Figure 1. As the water density decreases at 673 K, the limiting molar conductance of Cl^- ion shows a clear change of slope from the assumed linear dependence and that of OH^- have a clear maximum. While the behavior of the limiting molar conductance of Cl^- ion was well explained in the previous works,[3,4] the current study has not provided the correct trend for the limiting molar conductance of OH^- ion as a function of the water density at 673 K. The small limiting molar conductance of OH^- in the lower-density region in Figure 1 is apparently due to the lack of the Grotthuss mechanism because there is a very few water molecules in the second hydration shell around the OH^- at low water densities. If a certain decreasing amount of D by the Grotthuss chain mechanism with decreasing water density is added to the obtained D in Sim.2 in Figure 7, then the correct trend of D could be obtained. The Grotthuss chain mechanism is impossible in this study since the SPC/E water model is a rigid model and a dissociable water model such as the OSS2 model[19] is indispensable to study the Grotthuss chain mechanism. A molecular dynamics simulation study for the limiting molar conductance of OH^- ion at supercritical states is presently under study using the scaled OSS2 (sOSS2) model.[10]

Acknowledgments. This research was supported by Basic Science Research Program through the National Research Foundation of Korea (NRF) funded by the Ministry of Education, Science and Technology (NRF-2010- 0023062).

References

1. Zimmerman, G. H.; Gruszkiewicz, M. S.; Wood, R. H. *J. Phys. Chem.* **1995**, *99*, 11612.
2. Ho, P. C.; Palmer, D. A. *J. Solution Chem.* **1996**, *25*, 711.
3. Lee, S. H.; Cummings, P. T.; Simonson, J. M.; Mesmer, R. E. *Chem. Phys. Lett.* **1998**, *293*, 289.
4. Lee, S. H.; Cummings, P. T. *J. Chem. Phys*. **2000**, *112*, 864.
5. Berendsen, H. J. C.; Grigera, J. R.; Straatsma, T. P. *J. Phys. Chem.* **1987**, *91*, 6269.
6. Stillinger, F. H.; Weber, T. A. *Mol. Phys.* **1982**, *46*, 1325.
7. English, C. A.; Venables, J. A. *Proc. R. Soc. Lond. A* **1974**, *340*, 57.
8. Reid, R. C.; Prausnitz, J. M.; Sherwood, T. K. *The Properties of Liquids and Gases*; McGraw-Hill: New York, 1977.
9. Guissani, Y.; Guillot, B. *J. Chem. Phys.* **1993**, *98*, 8221.
10. Lee, S. H.; Rasaiah, J. C. *J. Chem. Phys.* **2011**, *135*, 124505.
11. Hoover, W. G.; Ladd, A. J. C.; Moran, B. *Phys. Rev. Lett.* **1982**, *48*, 1818.
12. Evans, D. J.; Hoover, W. G.; Failor, B. H.; Moran, B.; Ladd, A. J. C. *Phys. Rev. A* **1983**, *28*, 1016.
13. Evans, D. J. *J. Chem. Phys.* **1983**, *78*, 3297.
14. Evans, D. J. *Mol. Phys*. **1977**, *34*, 317.
15. Evans, D. J.; Murad, S. *Mol. Phys.* **1977**, *34*, 327.
16. Gear, W. C. *Numerical Initial Value Problems in Ordinary Differential Equations*; McGraw-Hill: New York, 1965.
17. Impey, R. W.; Madden, P. A.; McDonald, I. R. *J. Phys. Chem.* **1983**, *87*, 5071.
18. Lee, S. H.; Rasaiah, J. C. *J. Chem. Phys.* **1994**, *101*, 6964.
19. Ojamäe, L.; Shavitt, I.; Singer, S. J. *J. Chem. Phys.* **1998**, *109*, 5547.